LIMNOLOGY
and
OCEANOGRAPHY

ASLO

Limnol. Oceanogr. 63, 2018, S324–S339

doi: 10.1002/lno.10742

Evidence for regional nitrogen stress on chlorophyll *a* in lakes across large landscape and climate gradients

Christopher T. Filstrup [1]* Tyler Wagner,[2] Samantha K. Oliver [3] Craig A. Stow [4] Katherine E. Webster,[5] Emily H. Stanley,[3] John A. Downing[1]

[1]Large Lakes Observatory and Minnesota Sea Grant, University of Minnesota Duluth, Duluth, Minnesota
[2]U.S. Geological Survey, Pennsylvania Cooperative Fish and Wildlife Research Unit, Pennsylvania State University, University Park, Pennsylvania
[3]Center for Limnology, University of Wisconsin, Madison, Wisconsin
[4]Great Lakes Environmental Research Laboratory, National Oceanic and Atmospheric Administration, Ann Arbor, Michigan
[5]Department of Fisheries and Wildlife, Michigan State University, East Lansing, Michigan

Abstract

Nitrogen (N) and phosphorus (P) commonly stimulate phytoplankton production in lakes, but recent observations from lakes from an agricultural region suggest that nitrate may have a subsidy-stress effect on chlorophyll *a* (Chl *a*). It is unclear, however, how generalizable this effect might be. Here, we analyzed a large water quality dataset of 2385 lakes spanning 60 regions across 17 states in the Northeastern and Midwestern U.S. to determine if N subsidy-stress effects on phytoplankton are common and to identify regional landscape characteristics promoting N stress effects in lakes. We used a Bayesian hierarchical modeling framework to test our hypothesis that Chl *a*–total N (TN) threshold relationships would be common across the central agricultural region of the U.S. ("the Corn Belt"), where lake N and P concentrations are high. Data aggregated across all regions indicated that high TN concentrations had a negative effect on Chl *a* in lakes with concurrent high total P. This large-scale pattern was driven by relationships within only a subset of regions, however. Eight regions were identified as having Chl *a*–TN threshold relationships, but only two of these regions located within the Corn Belt clearly demonstrated this subsidy-stress relationship. N stress effects were not consistent across other intense agricultural regions, as we hypothesized. These findings suggest that interactions among regional land use and land cover, climate, and hydrogeology may be important in determining the synergistic conditions leading to N subsidy-stress effects on lake phytoplankton.

The Law of the Minimum states that plant growth depends on the availability of the nutrient that is scarcest relative to the plant's need (van der Ploeg et al. 1999). In 1899, Karl Brandt was the first to apply this concept to algal biomass regulation by hypothesizing that algal growth in the oceans was nitrogen (N) limited (de Baar 1994). Whereas N commonly limits phytoplankton growth in the open ocean (Vitousek and Howarth 1991), phosphorus (P) commonly limits phytoplankton growth in inland freshwaters (Dillon and Rigler 1974; Jones et al. 1976), which has led to the P paradigm for mitigating cultural eutrophication of aquatic ecosystems (Schindler 1977). Historically, far less attention has been paid to the role of N in limiting primary productivity in lakes (but see Scott and McCarthy 2010), despite the documented occurrence of N and P co-limitation in some aquatic ecosystems (Elser et al. 1990; Bracken et al. 2015). Whether or not a resource has a positive effect on primary production also depends on the abundance of that resource, however. Certain resources can have a stimulatory effect on primary productivity until a threshold concentration is reached, beyond which that resource negatively affects primary productivity, thereby displaying a "subsidy-stress gradient" (*sensu* Odum et al. 1979). For example, phytoplankters require adequate light to perform photosynthesis, although too much light, especially ultraviolet radiation, can inhibit their photosynthetic machinery and impede growth (Marwood et al. 2000; Staehr et al. 2016).

In addition to light, N may switch from serving as a subsidy to a stress on phytoplankton depending on its absolute concentration and its speciation. While both ammonium and nitrate are assimilated into phytoplankton biomass,

*Correspondence: filstrup@d.umn.edu

Additional Supporting Information may be found in the online version of this article.

therefore providing a subsidy, high concentrations of either species can also be harmful to phytoplankton. Occurrences of low phytoplankton biomass or growth in high macronutrient regions of the ocean or in estuaries were demonstrated to be caused by limitation by other resources (e.g., iron, light) or toxicity from anthropogenic compounds (Martin and Fitzwater 1988; Yoshiyama and Sharp 2006), although Yoshiyama and Sharp (2006) also speculated that high ammonium concentrations could have suppressed growth. In northern San Francisco Bay estuary, ammonium uptake by phytoplankton was reduced under high ammonium concentrations downstream of a wastewater treatment plant, resulting in a 60% decline in primary productivity (Parker et al. 2012). The physiological pathways by which high ammonium concentrations can suppress growth are fairly well known, especially in diatoms, and include repression of nitrate uptake and assimilation, enhanced photorespiration, accumulation of reactive oxygen species (ROS), and failure of nitrate- and nitrite-reductase dissipatory pathways (Glibert et al. 2016). Additionally, nitrate can undergo photolysis in surface waters to produce various ROS (e.g., $^{\bullet}NO_2$, $^{\bullet}OH$, and $^1O_2$) that are capable of oxidizing diverse organic compounds (Zafiriou 1974; Salin 1988; Vione et al. 2006). Production of ROS is not exclusive to nitrate photolysis and can also be produced by excited triplet state dissolved organic matter (^{3}DOM*), although nitrate is the predominate source under high nitrate conditions (Takeda et al. 2004; Vione et al. 2006).

Despite a well-developed mechanistic basis for suppression of phytoplankton growth and biomass under high N regimes, few studies have empirically demonstrated N stress effects on phytoplankton in lakes. High nitrate and high ammonium additions can reduce photosynthetic yield and growth within monocultures of different phytoplankton taxa, including *Microcystis aeruginosa* (Dai et al. 2012; Peng et al. 2016). In lake mesocosm experiments using natural phytoplankton communities under ambient high P conditions, diatom and cryptophyte biomass decreased in ammonium-enriched treatments, although total phytoplankton biomass increased overall in these treatments (Donald et al. 2013). More recently, a study from an intensively-managed agricultural region demonstrated a threshold relationship between phytoplankton biomass, whether measured as chlorophyll *a* (Chl *a*) or phytoplankton biovolume, and total N (TN) for lake observations with concurrent high total P (TP) concentrations (> 100 μg L^{-1}; Filstrup and Downing 2017). In these lakes, nitrate comprised nearly all of the TN for observations exceeding the TN threshold (2.9 mg L^{-1}), causing the authors to speculate that accumulation of ROS from nitrate photolysis may have negatively affected Chl *a*. This conclusion was reached after refuting other potential mechanisms that could produce similar Chl *a*–nutrient relationships (i.e., resource limitation shifts, cellular Chl *a* content fluctuations, phytoplankton composition changes, zooplankton grazing pressure), although there was some support for a seasonal signal underlying this relationship. Although the previously documented relationship implies that phytoplankters are stressed under high nitrate, high P regimes, the lack of empirical studies demonstrating this relationship despite high N and P concentrations in lakes worldwide suggests that there may be other factors interacting with high nitrate concentrations that lead to the expression of N stress effects.

Regional differences in land use and land cover (LULC), hydrology, and climate can create differences in the forms, ratios, and timing of limiting nutrients delivered to freshwater ecosystems, which may influence phytoplankton subsidy-stress responses. Regional variation in landscape features can create spatial variability in Chl *a*–limiting nutrient relationships, potentially by modifying bioavailability of nutrients or underwater light climate (Wagner et al. 2011; Filstrup et al. 2014). In particular, agricultural land use can greatly modify natural biogeochemical and hydrologic cycles in regions. Nutrient amendments to croplands and manure applications to croplands and pasturelands can decouple N and P cycles, thereby altering the relative proportion of N to P (N : P) delivered to receiving waters depending on the type of agriculture (Arbuckle and Downing 2001). N fertilizer applications to croplands can produce nitrate-enriched runoff and subsurface drainage waters (Gentry et al. 1998; Jaynes et al. 2001; Stanley and Maxted 2008). Additionally, hydrologic modifications to croplands can modify nutrient delivery, especially in poorly-drained regions. Subsurface tile drainage can comprise nearly half of total watershed discharge on a monthly basis and the majority of baseflow in streams within agricultural regions, thereby causing increased annual baseflow (Macrae et al. 2007; Schilling and Helmers 2008; King et al. 2014). The influences of subsurface tile drainage discharge are more pronounced in winter and spring when vegetation is sparse and evapotranspiration is low (Macrae et al. 2007; Vidon and Cuadra 2010), which may contribute to high nitrate export from croplands because it coincides with fertilizer applications. In addition to altering nutrient supply, croplands can influence nutrient bioavailability and underwater light climate, thereby producing complex responses of phytoplankton to nutrients (North et al. 2013). Finally, large water level fluctuations in reservoirs combined with changes in temperature and nutrients can influence overall phytoplankton abundance and composition, especially with respect to Cyanobacteria dominance (Yang et al. 2016, 2017), which may alter Chl *a*–nutrient relationships across regions.

Because agricultural lands can export large nitrate loads to receiving streams and the previously identified TN threshold concentration (2.9 mg L^{-1}) is within the range of TN values commonly observed in lakes in agricultural watersheds, intensively-managed agricultural regions, such as the "Corn Belt" of the U.S., may be susceptible to N subsidy-stress

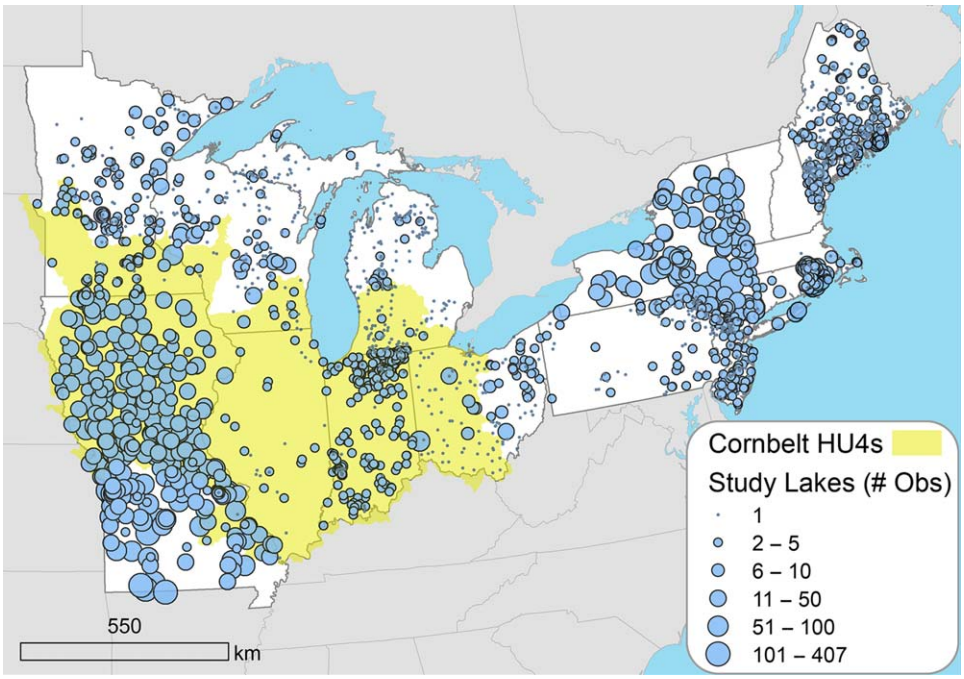

Fig. 1. Spatial extent of study region displaying number of observations per lake (circles) and approximate boundaries of the Corn Belt region (yellow).

relationships. Here, we analyzed a large dataset of lakes from diverse regions in the Northeastern and Midwestern U.S. (1) to determine if evidence consistent with subsidy-stress relationships exists along TN gradients across regions, (2) to determine whether these relationships are region-specific or widespread, and (3) to identify regional landscape characteristics promoting these effects if they are region-specific. We hypothesized that N stress effects would be detected in predominantly agricultural regions throughout the study extent, in which elevated N and P concentrations driven by these practices would contribute to phytoplankton stress responses. By examining empirical relationships between Chl *a* and nutrients across diverse regions at large spatial extents, we gain insight into the mechanisms responsible for producing N subsidy-stress relationships in lakes. Because N subsidy-stress relationships have never been explored at this scale, and given the evidence that various geophysical features within regions can alter Chl *a*–nutrient relationships, we also hypothesized that landscape features that can enhance nutrient delivery (e.g., geology, hydrology) or accumulation of ROS in the water column (e.g., nutrient and water pulses, intervals between storm events) would favor regional subsidy-stress responses.

Materials

Dataset description

To test our hypotheses, we analyzed the LAke multi-scaled GeOSpatial and temporal database (LAGOS-NE), as described by Soranno et al. (2015*a*), which is a subcontinental scale, integrated database of lake ecosystems. For our analyses, we used the following two modules: LAGOS-NE-$_{GEO}$ v1.05, which contained geospatial data (e.g., climate, LULC, hydrology, geology) on ~ 50,000 lakes with surface areas > 4 ha across 17 states in the Northeastern and Midwestern U.S., and LAGOS-NE-$_{LIMNO}$ v1.054.1, which contained water quality data on ~ 10,000 of these lakes (Fig. 1; Soranno et al. 2017). The spatial extent of the database covers large gradients in LULC, climate, and geology, making it ideal for testing our hypotheses. Additionally, the database includes lakes from the intensively managed, row-crop agricultural region of the U.S., also known as the "Corn Belt," where N amendments to croplands contribute to high N export rates from receiving streams (Fig. 1; Howarth et al. 1996). Regions within southwestern Minnesota, Iowa, Illinois, Indiana, and Ohio have been documented as the greatest contributors of nitrate to the Gulf of Mexico (David et al. 2010).

To maintain consistency with a previous study that demonstrated a Chl *a*–TN threshold relationship using some of the data included in this analysis, we used data from individual sampling events, rather than summarizing data by lake-year or by lake, despite potential concerns about sample independence. Filstrup and Downing (2017) commented that aggregating data by either season or by lake could obscure nonlinear Chl *a* responses to TN, which require numerous extreme TN observations to be adequately modeled and to maintain the statistical power to do so.

Additionally, summary statistics, such as sample averages, calculated from samples of differing sizes will have differing variances, requiring differential weighting in most common statistical analyses. The dataset was restricted to samples with concurrent measures of TN, TP, Chl *a*, and Secchi depth. In addition to TN concentrations reported by data providers, where data on individual N components were available, TN was calculated by summing total Kjeldahl nitrogen and nitrate + nitrite concentrations. The final dataset included observations from the upper mixed layer of the water column (i.e., epilimnion) recorded from May to September during 1990–2013, totaling 19,341 observations across 2385 lakes, with a median of two observations per lake (range: 1–407 observations; Fig. 1). In general, lakes with 20+ observations were sampled semi-monthly to monthly throughout the growing season for a portion of the dataset's temporal range, although several of the most frequently sampled lakes had sub-weekly observations potentially from different sampling locations within large natural and constructed lakes, such as reservoirs in Missouri. Lakes with the most observations tended to be concentrated in Missouri, New York, and Iowa. Lakes were distributed across 60 regions defined by U.S. Geological Survey 4-digit hydrologic units (HU-4) boundaries within the study extent.

The dataset we analyzed was constructed to answer questions on broad-scale regional controls on N stress across a larger and more geographically diverse spatial extent than that explored in Filstrup and Downing (2017). For example, the LAGOS-NE-$_{\text{LIMNO}}$ dataset (v1.054.1) included observations within 60 HU-4s within the Northeastern and Midwestern U.S. study extent, including seven overlapping Iowa state boundaries. The Iowa data included in our analyses comprised 105 lakes sampled between 2001 and 2009 ($n = 1531$ sampling events). These data were a subset of the more extensive dataset on 139 Iowa lakes representing a longer monitoring period (2001–2014) and more sampling events ($n = 4561$) analyzed by Filstrup and Downing (2017). Further, the availability of attributes, such as nitrate and ammonium concentrations, mixing depth, and phytoplankton and zooplankton biomass and composition, not available for all lakes in the LAGOS-NE database allowed Filstrup and Downing (2017) to address more focused mechanistic questions regarding relationships between Chl *a* and lake nutrients within a predominantly agricultural landscape.

Identifying stress responses and regions

To explore potential stress responses, we created contour plots to visualize Chl *a* response to both TN and TP following procedures used by Filstrup and Downing (2017). Local polynomial smoothing (2$^{\text{nd}}$-degree polynomial) was used to grid irregularly-spaced data in Surfer 8 software (Golden Software, Golden, Colorado, U.S.A.). Data were not filtered to remove or summarize "duplicates" (i.e., independent observations occupying the same *x*, *y*-coordinates) prior to analysis, which allowed for all Chl *a* values to be considered by smoothing algorithms. Contours were not extrapolated beyond the range of the dataset.

As we hypothesized that not all regions within our study extent would display subsidy-stress relationships, we first developed a method to exclude these "non-stress" regions from subsequent analyses so they did not bias our estimation of N stress thresholds. Because Chl *a*–nutrient relationships tend to be sigmoidal (McCauley et al. 1989; Prairie et al. 1989; Filstrup et al. 2014), we were concerned that modeling threshold responses for individual regions could differ depending on whether regions primarily had low or high nutrients; for the former, the threshold would likely occur at the bottom inflection point (i.e., acceleration phase *sensu* Filstrup et al. 2014), whereas the upper asymptote (i.e., deceleration phase) would serve as the threshold in the latter. To ensure that we were only comparing the upper threshold across regions, we first used Bayesian model selection to preliminarily identify regions as "stress regions" to be considered in subsequent subsidy-stress analyses.

The Bayesian choice model identified whether or not a change point model (i.e., a hockey stick model), which resembles a subsidy-stress relationship, would better describe Chl *a*–TN relationships for each region compared to a linear model. The hockey stick model was as follows:

$$y_i = \begin{cases} \beta_1 + \beta_2(x_i - \phi) + \epsilon_i & \text{if } x_i < \phi \\ \beta_1 + (\beta_2 + \delta)(x_i - \phi) + \epsilon_i & \text{if } x_i \geq \phi \end{cases} \quad (1)$$

where y_i is $\log_{10}$-transformed Chl *a*, x_i is the predictor variable ($\log_{10}$-transformed TN), β_1 and β_2 are the intercept and slope prior to the change point (ϕ), δ is the change in the slope after the change point, and ϵ_i is the error term independently and identically distributed as $N(0, \sigma^2)$. The linear model was:

$$y_i = \alpha + \gamma x_i + \epsilon_i \quad (2)$$

where y_i and x_i are as defined above, α is the intercept, γ is the slope, and ϵ_i is as defined above. Diffuse normal priors were used for β_x, δ, α, and γ, and uniform priors were used for σ and ϕ.

We used Markov chain Monte Carlo simulations within the program WinBUGS version 1.4 (Spiegelhalter et al. 2003) to compare the two models. Two parallel Markov chains with different starting values were simulated, in which the first 25,000 samples from a total of 40,000 iterations were excluded as burn-in. For the remaining samples, every other sample was retained. Model convergence was evaluated using the Gelman-Rubin convergence statistic ($\hat{r}$), where values < 1.1 indicate convergence. Additionally, we visually inspected trace plots and density plots of model parameters to further assess convergence.

Bayesian model selection was employed to select between the two candidate models. Model selection was achieved by

introducing a model indicator z to select either model 1, the linear model ($z = 1$), or model 2, the threshold model ($z = 0$). The introduction of the indicator variable allowed for the posterior frequency of selecting model 1 ($f = \mathrm{P}(z = 1|\mathrm{data})$, where a large value of f indicates preference for model 1. A Bernoulli prior was used for z, where $z \sim$ Bernoulli(0.5). We performed this analysis for each region separately.

For a region to be considered a potential stress region for subsequent analyses, the following a priori criteria had to be satisfied. (1) The posterior frequency (f) of selecting the linear model over the change point model had to be < 0.40. Although this posterior frequency criterion was somewhat arbitrary, the selection process was largely insensitive to this value as nearly all retained regions had much stronger preference for the change point model ($f < 0.15$). (2) The TN threshold had to be > 1 mg L^{-1} to avoid identifying regions in which the threshold could occur at the lower inflection point of a sigmoidal Chl *a*–TN relationship, as previously mentioned. (3) The post-threshold slope had to be negative to identify regions in which TN concentrations were stressful (i.e., had a negative effect) on Chl *a*. We were conservative in excluding regions where the post-threshold slope was smaller, but still positive, compared to the pre-threshold slope, which could have simply indicated shifting resource limitation. (4) At least 10% of observation within a region had to be greater than the regional TN threshold to systematically discard regions in which a small number of observations were driving the negative post-threshold slope (i.e., exclude potentially coincidental relationships).

Identifying landscape characteristics promoting N stress

For regions identified as stress regions by Bayesian model selection, we subsequently modeled Chl *a*–TN relationships using a Bayesian hierarchical threshold model, in which all model parameters were allowed to vary across regions. The hierarchical threshold model allowed for subsidy-stress relationships to be quantified at the population level (i.e., across all regions and considering all observations) and at the regional level (i.e., within each individual region). The Bayesian hierarchical threshold model was as follows:

$$y_i \sim N\left(\alpha_{j[i]} + \beta_{j[i]} x_i + \delta_{j[i]} \left(x_i - \phi_{j[i]}\right)_+, \sigma^2\right) \text{ for } i = 1 \ldots, n \quad (3)$$

$$\begin{pmatrix} \alpha_j \\ \beta_j \\ \delta_j \\ \phi_j \end{pmatrix} \sim MVN(\boldsymbol{\mu}, \Sigma) \text{ for } j = 1 \ldots J \quad (4)$$

$$\boldsymbol{\mu} = \left(\bar{\alpha}, \bar{\beta}, \bar{\delta}, \bar{\phi}\right) \quad (5)$$

where y_i is $\log_{10}$-transformed Chl *a*, x_i is the predictor variable ($\log_{10}$-transformed TN), and the spatially-varying (region-specific) parameters include the intercepts (α_j), regression slopes prior to the change point (β_j), change in regression slopes after the change points (δ_j), and the change points (ϕ_j). The index $j[i]$ indexes region j for observation i. The term $(x_i - \phi_{j[i]})_+$ is equal to $(x_i - \phi_{j[i]})$ if $x_i > \phi_j$, and 0 otherwise. The parameters $\bar{\alpha}, \bar{\beta}, \bar{\delta}, \bar{\phi}$ describe the threshold response across all regions (i.e., the population-average response). Diffuse normal priors were used for $\bar{\alpha}, \bar{\beta}, \bar{\delta}, \bar{\phi}$, and diffuse uniform prior for σ, and Σ was modeled using the scaled inverse-Wishart distribution (Gelman and Hill 2007).

The model was fit using the program Just Another Gibbs Sampler (Plummer 2012). Three parallel Markov chains with different starting values were simulated from a total of 1,000,000 iterations, of which the first 850,000 samples were excluded as burn-in. For the final 150,000 iterations, every fourth sample was retained. Model convergence was evaluated using $\hat{r}$, trace plots, and density plots of posterior distributions.

We considered LULC categories and climate and hydrogeology metrics to identify regional landscape characteristics promoting N stress in regions. Although we originally intended to predict regional threshold model parameters (i.e., threshold and post-threshold slope) as a function of landscape characteristics, the low number of stress regions did not provide the statistical power needed to do so. Therefore, we qualitatively compared landscape characteristics between "stress" and "non-stress" regions. Because water quality data were from 1990 to 2013, where possible, landscape characteristics were selected to correspond to this temporal range. Percent row-crop agriculture, pasture, and wetlands (woody + herbaceous) within regions were evaluated because of their previously documented influences on regional Chl *a*–nutrient relationships (Wagner et al. 2011; Filstrup et al. 2014). LULC data were obtained from the 2001 National Land Cover Dataset (Homer et al. 2007), which represented LULC characteristics most closely corresponding to the midpoint of our dataset's duration. Regional precipitation was represented as 30-yr normals (1981–2010) using PRISM data (PRISM Climate Group, Oregon State University, http://www.prism.oregonstate.edu, created 2004 February 04). Regional average runoff data were obtained from the U.S. Geological Survey (https://water.usgs.gov/GIS/metadata/usgswrd/XML/runoff.xml). We also considered atmospheric deposition of TN and nitrate because of its importance in determining nutrient limitation in some lakes, especially those removed from intense watershed modification and human activities (Bergström and Jansson 2006; Elser et al. 2009). Regional TN and nitrate deposition data from 2000 were obtained from the National Atmospheric Deposition Program (http://nadp.sws.uiuc.edu/ntn/annualmapsByYear.aspx). Data sources and LAGOS-NE-$_{GEO}$ database development are described in Soranno et al. (2015*a*).

Results

Identifying stress responses and regions

For individual sampling events, water quality conditions within the study extent spanned a broad trophic gradient,

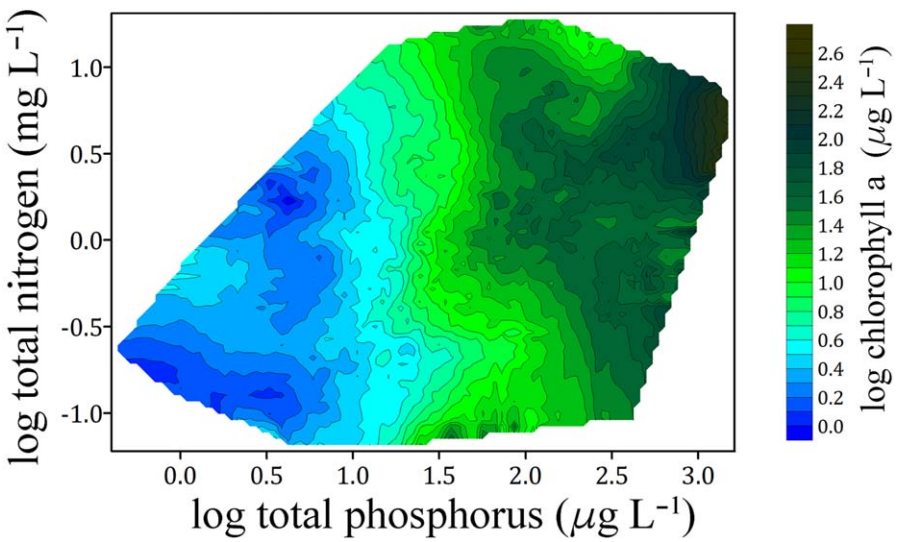

Fig. 2. Chl *a* (μg L^{-1}) contour plot on TN (mg L^{-1}) vs. TP (μg L^{-1}) space. Contours were created using 2nd-degree local polynomial smoothing of individual sample observations. All variables were $\log_{10}$-transformed.

with individual observations ranging widely in Chl *a* (< 0.1–743 μg L^{-1}), TN (0.06–20.57 mg L^{-1}), and TP (0.4–1623.0 μg L^{-1}). Consequently, average water quality conditions within regions ranged from low nutrient, low productivity regions to high nutrient, high productivity regions (Supporting Information Table 1). Median regional Chl *a* (18.4 μg L^{-1}), TN (0.8 mg L^{-1}), and TP (50.3 μg L^{-1}) concentrations suggest that a large proportion of lakes were eutrophic in a majority of regions. Due to regional differences in nutrient concentrations, average phytoplankton growth conditions ranged from stoichiometrically balanced to P-deficient growth conditions (TN : TP by atoms: 30.8–170.9), with most regions ($n = 46$ of 60 regions) displaying P-deficient growth conditions (Supporting Information Table 1).

When considering all lakes across the study's spatial extent, the relationship between Chl *a* and TN and TP diverged depending on the relative availability of these nutrients. At TP < 100 μg L^{-1} (2.0 as $\log_{10}$-transformed value), Chl *a* did not respond to changing TN across a two order-of-magnitude TN gradient, as demonstrated by the nearly vertical Chl *a* contours (Fig. 2). In contrast, increased TN was accompanied by increased Chl *a* when TP exceeded 100 μg L^{-1}. The highest Chl *a* concentrations were not found for observations with the highest TP and TN concentrations, as predicted by N and P co-limitation paradigms, but rather occurred when TP was high and TN moderate. When TP exceeded 100 μg L^{-1}, Chl *a* displayed a unimodal response to TN, in which Chl *a* was positively related to TN at low TN intervals and negatively related to TN at high TN intervals (Fig. 2).

We used Bayesian model selection to identify potential stress regions defined by those for which change point models better fitted regional Chl *a*–TN relationships compared to linear models. Of the 60 regions included in this study, only eight were identified as stress regions (Fig. 3). These regions had strong preferences for the change point model compared to the linear model, with linear model preference values below 0.15 for seven regions. In these seven regions, the percentage of observations greater than or equal to regional TN thresholds ranged from 13.5% to 63.0%, with two regions in Iowa having the highest percentages. Due to a small sample size, it was more difficult to discern between the two models (linear model preference = 0.28) for the other potential stress region (HU4_50), in which only six observations had TN concentrations greater than the regional TN threshold. Overall, these eight regions were preliminarily classified as stress regions and were retained in subsequent analyses.

Identifying landscape characteristics promoting N stress

When aggregating observations across the eight stress regions, Chl *a* displayed a threshold relationship with TN (Fig. 4), with concentrations increasing with TN below the TN threshold, but decreasing above 1.81 mg L^{-1} (0.26 as $\log_{10}$-transformed value). This TN threshold estimate had 95% credible intervals (CI) of 0.87–3.82 mg L^{-1}. Population average pre- and post-threshold slopes were estimated at 1.44 (95% CI: 0.99, 1.88) and −0.58 (95% CI: −1.21, −0.01), respectively. Overall, 24.2% ($n = 906$) of observations had TN concentrations equal to or exceeding this population average TN threshold.

When examining individual region parameter estimates, Chl *a*–TN relationships were weaker for most of these eight regions and TN thresholds varied from 1.05 mg L^{-1} to 3.66 mg L^{-1} (0.0–0.6 as $\log_{10}$-transformed values; Supporting Information Table 2; Fig. 5). Due to a small number of total observations or a low percentage of observations above

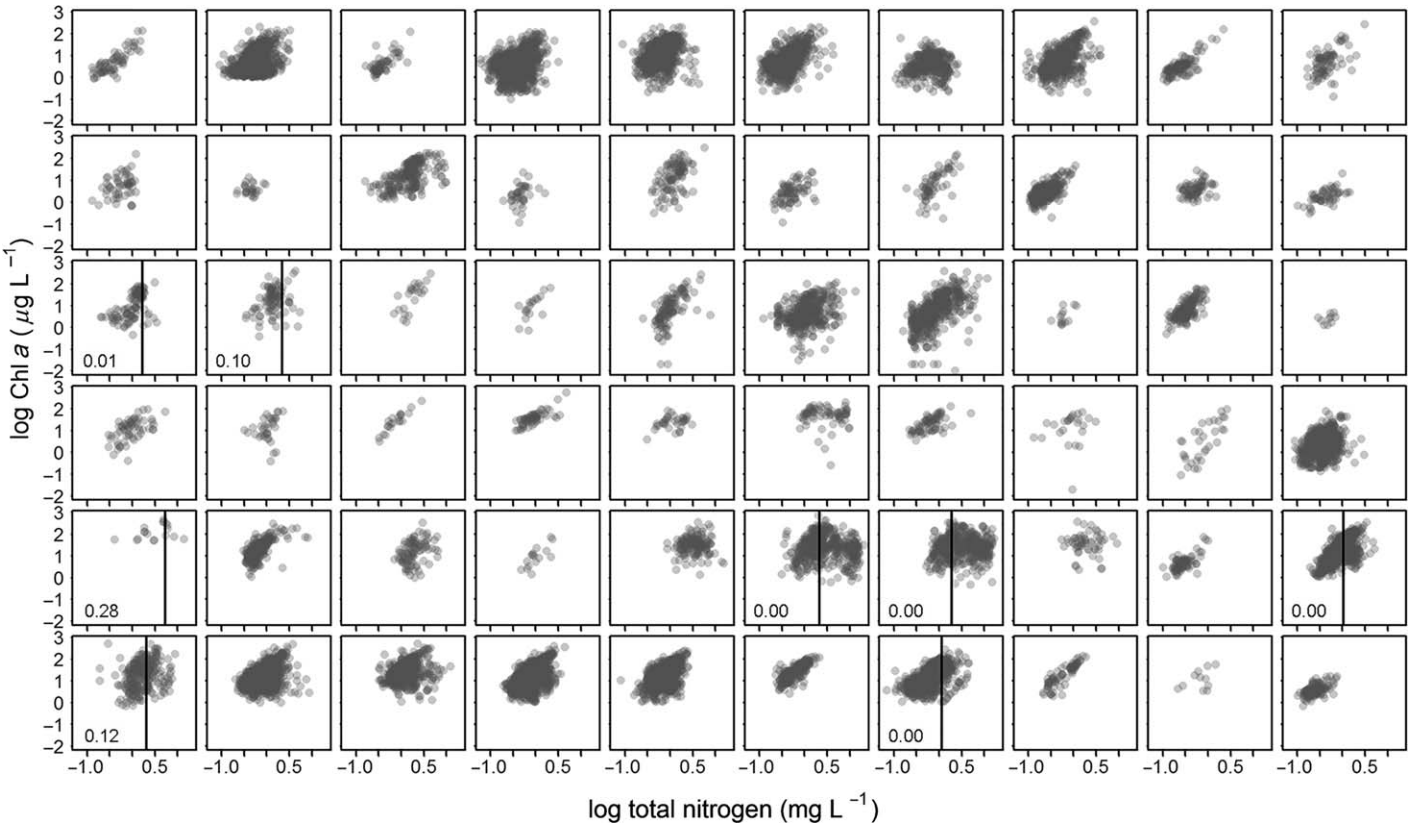

Fig. 3. Chl *a*–TN relationships for each region located within this study's spatial extent. For regions that met the criteria of stress regions, vertical lines representing the TN change point and values (lower left corner) indicating preference for the linear model (low values = change point model preference) are displayed. Markers representing individual lake observations are transparent, so darker clusters represent overlapping markers. Variables were $\log_{10}$-transformed.

regional thresholds for most regions, uncertainty in modeled relationships was often high either across the entire TN range (e.g., Fig. 5c) or across TN concentrations greater than regional TN thresholds (e.g., Fig. 5b). Additionally, three regions (Fig. 5b,c,f) had 95% CI for post-threshold slope estimates overlapping zero (Supporting Information Table 2). In contrast, two regions (Fig. 5d,e) had tighter confidence intervals across their entire TN ranges, including those for their post-threshold slope estimates (Supporting Information Table 2), due to a more equitable distribution of observations before and after regional TN thresholds. TN thresholds were 2.06 mg L^{-1} and 1.85 mg L^{-1} for these two regions, respectively. These findings suggest that although eight regions were preliminarily identified as potential stress regions, for the remaining six, we either have not captured high TN events and could not obtain precise parameter estimates, or high TN events did not occur in these regions and neither the change point model nor the linear model was an appropriate approximation of Chl *a*–TN relationships. Only two regions appeared to be driving the Chl *a*–TN relationships at the population level (i.e., across all stress regions; Fig. 4). Both of these regions had > 300 observations ($n = 313$ and 314, respectively) of high TN concentrations exceeding the estimated change point that contributed to the increased precision of the post-change point slope for the population-average estimate compared to the region-specific estimates. Additionally, relationships from these two regions suggest that TN concentrations exceeding 2 mg L^{-1} (0.30 as $\log_{10}$-transformed value) may negatively influence Chl *a* concentrations.

The eight stress regions were restricted to the western portion of our study extent and were located along the entire north-south gradient of this study (Fig. 6). These regions differed widely in their LULC characteristics for row-crop agriculture (4.5–73.7%), pasturelands (4.7–27.1%), and wetlands (1.3–26.2%). Counter to our hypothesis, stress regions were located within some, but not all, of the regions with the highest row-crop agriculture land use (Fig. 6a). Because of the different LULC characteristics for stress regions, average nutrient concentrations for lakes within the stress regions varied from medium to high (Fig. 7). With the exception of the southern-most stress region, average regional TN concentrations in stress regions ranged from 0.96 mg L^{-1} to 4.24 mg L^{-1}, but stress regions were not exclusive to the

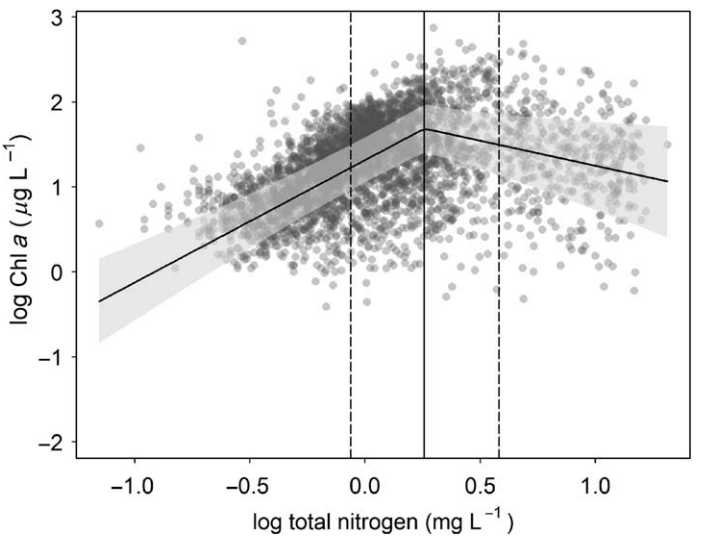

Fig. 4. Population-level change point model of Chl *a*–TN relationship for lakes across the eight regions identified as stress regions. Black line represents the median change point model fit to lake observations (individual markers). Gray shaded region represents 95% credible region. Solid vertical black line is the population-level average TN threshold, whereas dashed vertical black lines are the 95% confidence intervals around the threshold estimate. Markers are transparent, so darker clusters represent overlapping markers. Chl *a* (μg L^{-1}) and TN (mg L^{-1}) were $\log_{10}$-transformed.

highest TN regions (Supporting Information Table 1; Fig. 7a). Similarly, stress regions were not restricted to the highest TP regions (Fig. 7b). Average regional TP concentrations in stress regions ranged from 50.5 μg L^{-1} to 443.1 μg L^{-1}, although they fell within the upper half of regional TP concentrations across all regions (median: 50.3 μg L^{-1}; Supporting Information Table 1).

Regional landscape characteristics varied less for the two regions that demonstrated the strongest subsidy-stress relationships. These regions had two of the six highest percentages for row-crop agriculture (66.6% and 69.7%), percentages of pasturelands within the upper 50th percentile (7.5% and 12.3%), and low percentages of wetlands (< 3.0% each) compared to the other six "stress" regions and all other regions (Fig. 6). Average nutrient concentrations likewise were high for these two regions (Fig. 7), with average TN concentrations > 4.00 mg L^{-1}, ranking 2nd and 3rd overall, and average TP concentrations > 98 μg L^{-1} (Supporting Information Table 1). Despite relatively high TP concentrations, these regions had the two highest TN : TP ratios of any region included in this study (Supporting Information Table 1; Fig. 7c). In contrast, other regions with high TP concentrations commonly had low TN : TP ratios (c.f., Fig. 7b,c).

Because the spatial distribution of stress regions countered hypotheses based solely on LULC, we also considered regional variability in climate, hydrology, and atmospheric N deposition as potential factors promoting N stress regions. Excluding the southern-most stress region, stress regions were located within medium to low precipitation regions compared to other regions within the study extent, with the two distinct stress regions having low mean annual precipitation (Fig. 8a). Because variability in annual runoff rates largely followed that of mean annual precipitation, these two stress regions also had among the lowest annual runoff rates. Atmospheric deposition of TN was commonly lowest along the western portion of our study extent, where our stress regions occurred, and greatest further east into Michigan, Ohio, Pennsylvania, and New York (Fig. 8b). Atmospheric deposition of nitrate followed similar spatial patterns, but tended to make up an increasing percentage of TN deposition moving from west to east.

Discussion

In this study, we found evidence consistent with N subsidy-stress effects on Chl *a* within individual regions across a broad spatial extent. Counter to expectations, however, subsidy-stress relationships were not widespread in agricultural regions, but were limited to two of the most intense agricultural regions considered in this study, which included the study extent of Filstrup and Downing (2017). Because these two regions contributed a majority of high nutrient lake observations, patterns between Chl *a* and nutrients were similar between the two studies, with Chl *a* displaying little response to TN when TP concentrations were below 100 μg L^{-1} and a unimodal response to TN when TP exceeded 100 μg L^{-1} in this study (Fig. 2). Overall, this general pattern between Chl *a* and nutrients agrees with Liebig's Law of the Minimum and nutrient limitation theory by demonstrating that N concentrations have little effect on phytoplankton biomass when P concentrations are likely to be limiting. Further, this finding suggests that Chl *a* predictive models can be improved by including TN and TN : TP in addition to TP, as has been previously demonstrated (Smith 1982; Canfield 1983; Prairie et al. 1989), although the importance and direction of their effect on Chl *a* may depend on the absolute concentrations of both N and P. Additionally, the TN threshold of 1.81 mg L^{-1} found in this study was slightly lower, but of similar order-of-magnitude, to the previously-demonstrated threshold (2.93 mg L^{-1}; Filstrup and Downing 2017), likely resulting from the majority of high nutrient observations being from regions contained within the overlapping spatial extent of the two studies.

In contrast to previous empirical studies demonstrating either log-linear or log-sigmoidal relationships between Chl *a* and TN (Sakamoto 1966; Canfield 1983; Prairie et al. 1989), our study demonstrated a Chl *a* threshold response to TN (Fig. 4). The variation in the form of these empirical relationships may be due to differences in the ranges and distributions of TN concentrations considered in each study, as well as the manner in which data were aggregated. For

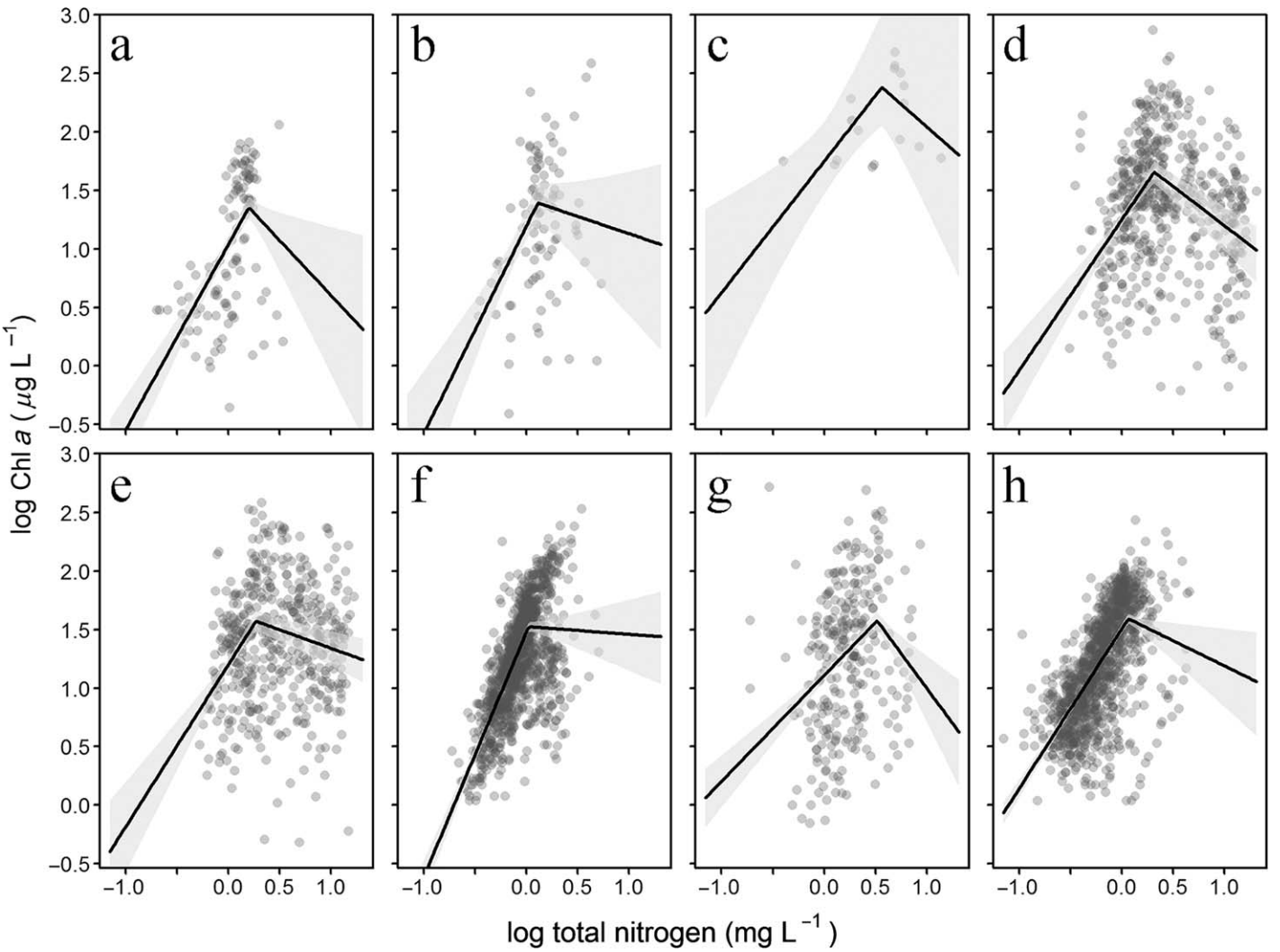

Fig. 5. Region-specific change point models of Chl *a*–TN relationships for lakes across the eight regions identified as stress regions. Regions are (a) HU4_32, (b) HU4_33, (c) HU4_50, (d) HU4_56, (e) HU4_57, (f) HU4_60, (g) HU4_61, and (h) HU4_67. Black line represents the median change point model fit to lake observations (individual markers). Gray shaded region represents 95% credible region. Markers are transparent, so darker clusters represent overlapping markers. Chl *a* (μg L^{-1}) and TN (mg L^{-1}) were $\log_{10}$-transformed.

example, the two studies displaying log-linear relationships had lower TN concentration gradients, achieving maximum TN concentrations of 5–6 mg L^{-1} (Sakamoto 1966; Canfield 1983), whereas the studies displaying nonlinear relationships on log-log scales had maximum TN concentrations exceeding 10 mg L^{-1} (Prairie et al. 1989; this study). While the dataset analyzed by Prairie et al. (1989) only contained one observation exceeding 10 mg L^{-1} TN, the dataset analyzed here contained 136 observations with TN greater than 10 mg L^{-1} and the upper quartile of TN concentrations exceeding 1 mg L^{-1}. The rarity of high TN data in the former study likely resulted from aggregating data by lake-wide averages, whereas using observational data (this study) may be required to produce enough high TN observations to identify N stress effects. Although the TN threshold was estimated at 1.81 mg L^{-1} with TN concentrations commonly exceeding this threshold in regions throughout the study extent (Figs. 3, 4), this inter-study comparison suggests that numerous observations with high TN conditions (> 10 mg L^{-1}) are required to reveal N stress effects on Chl *a* (i.e., model the negative arm of the threshold model). Further, the two stress regions that most clearly displayed threshold relationships had the largest proportions of observations beyond their regional TN thresholds, as well as having the highest number of high TN observations (Fig. 5d,e). The rarity of high TN observations from other agricultural regions may be one of the reasons why N stress regions were not as common as we anticipated.

Additionally, the occurrence of N stress regions was not simply a question of agricultural land use, as we originally hypothesized. N subsidy-stress effects on Chl *a* were not common within other predominantly agricultural regions

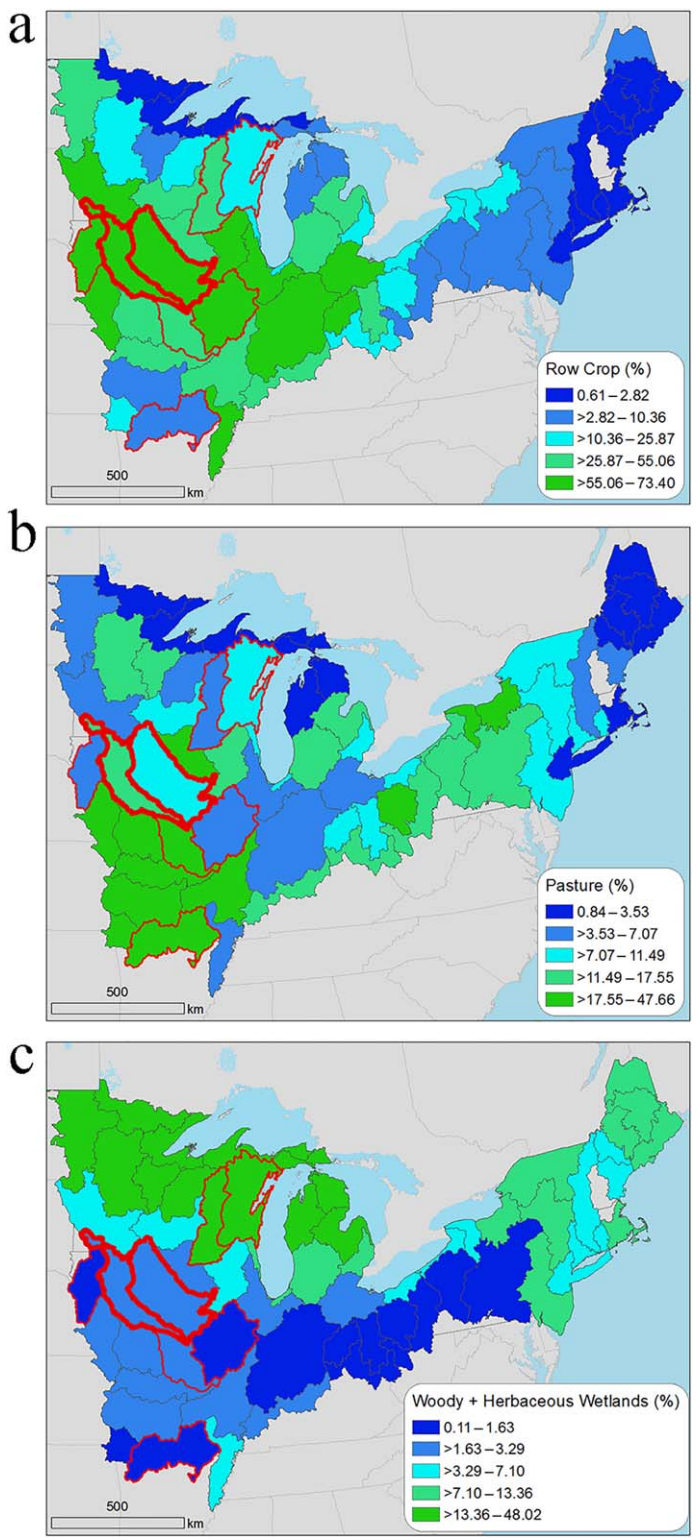

Fig. 6. Percent LULC by region for (**a**) row crop agriculture, (**b**) pasturelands, and (**c**) woody and herbaceous wetlands. Black boundaries represent individual regions. Red boundaries identify regions selected as stress regions by the Bayesian choice model, whereas thick red boundaries identify the two regions that strongly demonstrated subsidy-stress relationships. Values were categorized by quintiles for mapping.

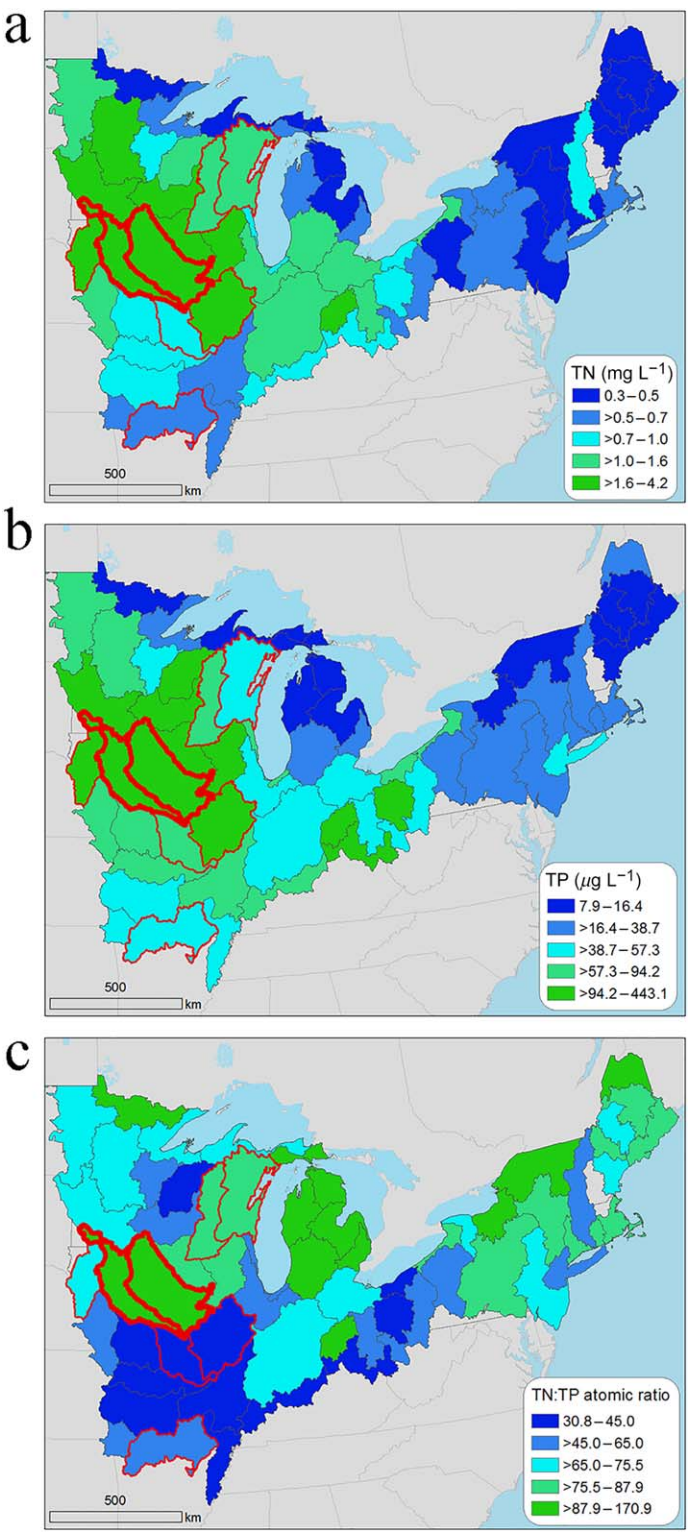

Fig. 7. Regional average concentrations for (**a**) TN (mg L^{-1}) and (**b**) TP (μg L^{-1}) and (**c**) regional average ratios of TN-to-TP (TN : TP; by atoms). Black boundaries represent individual regions. Red boundaries identify regions selected as stress regions by the Bayesian choice model, whereas thick red boundaries identify the two regions that strongly demonstrated subsidy-stress relationships. Values were categorized by quintiles for mapping.

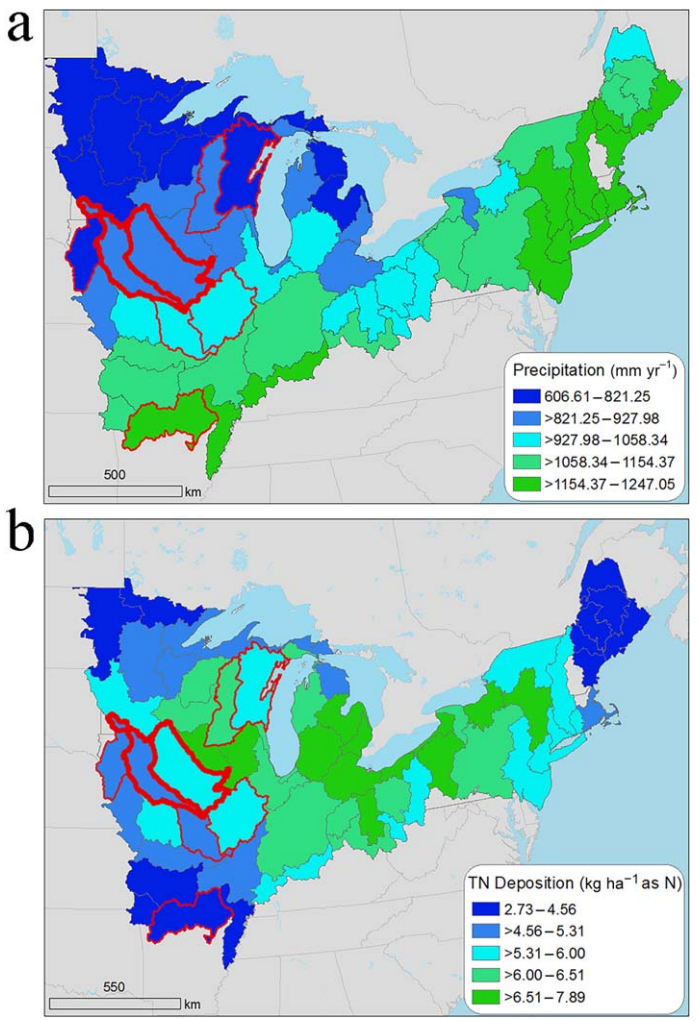

Fig. 8. Regional values for (**a**) mean annual precipitation (mm yr^{-1}) and (**b**) atmospheric TN deposition for the year 2000 (kg ha^{-1}). Black boundaries represent individual regions. Red boundaries identify regions selected as stress regions by the Bayesian choice model, whereas thick red boundaries identify the two regions that strongly demonstrated subsidy-stress relationships. Values were categorized by quintiles for mapping.

located within the Corn Belt (Fig. 6a), although the two regions that were primarily responsible for creating the Chl *a*–TN threshold relationship observed across all eight stress regions had high proportions of agricultural land use (Figs. 4, 5). Combined with the fact that these two stress regions had the 2nd and 3rd greatest regional average TN concentrations, these findings suggest that rather than simply examining proportional coverage of agricultural practices, more detailed information on the practices themselves, along with a greater number of observations per lake collected throughout the growing season, are required to detect the effect of high N concentrations on Chl *a*. For example, the form of dissolved inorganic N (DIN) is also important if N stress effects on phytoplankton result from accumulation of nitrate-derived ROS in the water column (Takeda et al. 2004; Vione et al. 2006), as was hypothesized by Filstrup and Downing (2017). In regions where anhydrous ammonia amendments to croplands are large, lakes can have high nitrate concentrations within the water column due to oxidation of ammonia within soils and receiving waters, whereas high urea concentrations may be more common in lakes where manure or other urea-based fertilizer applications predominate (Glibert et al. 2006). For example, Cooke and Prepas (1998) found that nitrate dominated DIN composition in cropland watersheds compared to dominance of ammonium in mixed agricultural watersheds. Although high ammonium concentrations can also suppress phytoplankton growth (Glibert et al. 2016), high TN concentrations in the two stress regions were almost exclusively driven by nitrate + nitrite (Filstrup and Downing 2017).

The occurrence of Chl *a*–TN threshold relationships under concurrent high TP regimes (> 100 μg L^{-1}) suggests that TN and TP were interacting to determine whether high N concentrations provided a subsidy or induced a stress in phytoplankters (Fig. 2). Different types of agriculture can have differing effects on natural biogeochemical cycles, thereby modifying the relative export of N and P to receiving streams. For example, lakes in watersheds dominated by row-crop agriculture tend to have high TN : TP ratios, whereas lakes in watersheds dominated by pasturelands tend to have low TN : TP ratios (Downing and McCauley 1992; Arbuckle and Downing 2001). Despite having amongst the highest TP concentrations, the two stress regions maintained the two highest TN : TP ratios of any region included in this study (Supporting Information Table 1; Fig. 7c), indicating that anhydrous ammonia applications were outpacing P export from croplands (Dinnes et al. 2002). In contrast, other regions with medium to high TP concentrations located within the Corn Belt commonly had relatively low TN : TP ratios (c.f., Fig. 7b,c). This finding implies that N serves as a subsidy to phytoplankters when systems are under balanced or N-deficient growth conditions because N is in short supply relative to P and therefore is assimilated into phytoplankton biomass, whereas under strict P-deficient growth conditions, N is present in excess relative to growth requirements and therefore can accumulate in the water column. The regional average TN : TP ratios for the two stress regions (171 and 155 by atoms) were more than triple the threshold value demarcating P-deficient growth conditions (50 by atoms; Guildford and Hecky 2000). This finding suggests that regions where N amendments to croplands result in high nitrate concentrations in receiving water that also have high enough N : P to maintain strict P-deficient growth conditions are most susceptible to displaying N stress effects.

Combined with surplus nutrients on croplands, the movement of nutrients from the landscape to receiving streams, which can be influenced by interactions among LULC, climatic patterns, and hydrology, may be important in

identifying N stress regions. Previous studies have demonstrated the importance of lake landscape position, hydrogeomorphology, and watershed permeability in helping determine lake water quality responses to watershed LULC and anthropogenic activities (Martin and Soranno 2006; Bremigan et al. 2008; Fraterrigo and Downing 2008; Soranno et al. 2015*b*). Clustering of the eight stress regions with respect to an east-west precipitation gradient, rather than a strict LULC gradient (Figs. 6, 8a), suggests that runoff and lake hydrologic connectivity contributed to the spatial distribution of N stress regions. Because most stress regions were also located within medium to low atmospheric TN deposition regions (Fig. 8b), high TN concentrations likely originated from N export from the surrounding terrestrial landscape. Counterintuitive to these claims, most N stress regions had medium to low mean annual precipitation rates for our study region (Fig. 8a), possibly suggesting that the intensity, frequency, or timing of nutrient delivery or all three may contribute to mechanisms underlying N stress. Experimental studies have previously demonstrated that pulsed delivery of nutrients modify phytoplankton community responses to nutrients compared to steady-state delivery (Sommer 1985; Suttle et al. 1987). In regions with highly permeable landscapes, such as intensively-managed agricultural regions with tile drainage (Fraterrigo and Downing 2008), infrequent pulses of high nitrate loads to lakes may create conditions conducive to accumulation of ROS and resulting stress responses by phytoplankters: rapid increases in nitrate to high water column concentrations may undergo photolysis to produce ROS, which accumulate in the water column and react with dissolved organic matter (DOM) and phytoplankton for extended periods before the next flushing event. Alternatively, water level fluctuations resulting from large runoff events can alter phytoplankton biomass and composition (Yang et al. 2016, 2017), potentially modifying phytoplankton response to N stress. These findings may also indicate that the timing of high nitrate pulses, which often coincide with spring storms following fertilizer and herbicide applications (Gaynor et al. 1992; Becher et al. 2001), could decouple Chl *a* response to high TN concentrations through negative effects of herbicides on phytoplankton (DeNoyelles et al. 1982; Bester et al. 1995). Further evidence would be needed to support these hypotheses, however.

Although six stress regions did not have enough observations with high TN concentrations to clearly define potential Chl *a*–TN threshold relationships, the remaining two stress regions may provide insight into the optimal combination of conditions that make systems vulnerable to N stress. Large N amendments to croplands that are heavily tile drained can result in pulses of high nitrate concentrations to receiving streams and lakes (Gentry et al. 1998; Jaynes et al. 2001; David et al. 2010). These high nitrate loads help maintain strict P-deficient growth conditions despite high P concentrations in lakes, which allows high nitrate concentrations to be maintained in the water column for extended periods. Concurrently, high P concentrations stimulate phytoplankton productivity that may increase interactions among various ROS and phytoplankters, potentially allowing them to interact for extended periods between storm-driven flushing events. In lakes within these two stress regions, DOM primarily originates from autochthonous sources (A. Morales-Williams pers. comm.), potentially supporting the hypothesis that either Chl *a* or phytoplankton cell lysis can result from interactions with ROS. These same factors may also reduce the duration in which N is stressful to phytoplankters. DOM has been demonstrated to be an effective scavenger of ROS (Brezonik and Fulkerson-Brekken 1998), so ROS would be increasingly scavenged as more phytoplankton cells are lysed. Additionally, droughts can cause some systems in agricultural watersheds to shift to N-limitation (Hayes et al. 2015), which is hypothesized to cause nitrate to shift from a stress to a subsidy with increasing time since the last flushing event. Combined with chlorophyll's protective systems against oxidative stress (Salin 1988), these opposing mechanisms suggest that N stress effects are ephemeral and highly dynamic in both space and time, and therefore require further study.

In addition to considering stress induced by accumulation of nitrate-derived ROS as a potential mechanism underlying these relationships, we tested whether seasonal effects based on phytoplankton phenology could be influencing the high nutrient, low Chl *a* region. Filstrup and Downing (2017) found that high TN concentrations occurred more frequently in early summer, potentially occurring before phytoplankton biomass was able to develop under more favorable temperature and light conditions in mid- to late summer. In agricultural regions, fertilizer applications in spring can lead to high N concentrations in receiving streams, especially when followed by large runoff events (Becher et al. 2001). Because we lacked comprehensive data on phytoplankton composition and therefore could not directly evaluate phytoplankton seasonal succession, we compared cumulative frequency distributions of sampling events among regions. If this mechanism was primarily responsible for producing the high nutrient, low Chl *a* region, then sampling events for N stress regions would be expected to begin earlier in the year than other regions. Cumulative frequency distributions of sampling events do not support this mechanism (Supporting Information Fig. 1). Sampling events for stress regions began around the same time of year as those for other regions, and the two strongest stress regions had sampling that started later in the year than most other regions. Additionally, sampling for these two regions concluded before most other regions, meaning that their sampling timeframe was more compressed than for other regions. As a result, phytoplankton communities would be expected to show a weaker seasonal signal in the strongest stress regions, especially compared to higher latitude regions. Despite the compressed

timeframe, these two regions had observational data extending through late August, which likely covered the period for which peak Chl *a* concentrations would be observed. These findings suggest that phytoplankton phenology was not driving the N subsidy-stress effects observed in this study.

Finally, this study highlights important lessons to be considered when performing macrosystems ecology research or large empirical analyses using secondary datasets. Had we examined Chl *a*–nutrient relationships by aggregating all data, we would have incorrectly concluded that stress regions were common throughout our study extent, when in fact they were largely driven by relationships within two regions (c.f., Fig. 2 vs. Fig. 5). By interrogating these overall relationships at the regional scale, we were able to constrain estimates of TN thresholds and develop a more accurate model of landscape characteristics promoting N stress first by comparing the eight regions preliminarily identified as stress regions by Bayesian model selection to all other regions and subsequently by comparing the two strongest stress regions to the other six weaker stress regions. Several recent studies have demonstrated the importance of incorporating regional-scale drivers, as well as regional-scale landscape heterogeneity, when examining water quality relationships and ecosystem functioning at broad spatial extents (e.g., Filstrup et al. 2014; Cheruvelil et al. 2017; Lapierre et al. 2017).

Conclusions

Our findings suggest that N can switch from providing a subsidy to inducing a stress in phytoplankton from nutrient-rich lake regions at N concentrations that are commonly observed in worldwide lakes, but interactions among LULC, climate, and hydrogeology may influence whether or not N stress effects occur within a particular region. Because N stress effects were rare within our study extent, we were able to deduce the regional landscape characteristics under which N stress effects are likely to occur, which seem to align with anticipated conditions under various global change scenarios. Agricultural intensification, especially increased N amendments to croplands, to meet growing global demand for food, fiber, and shelter is likely to increase nitrate export to receiving waters (Cooke and Prepas 1998; Jaynes et al. 2001), thereby supplying the high nitrate concentrations needed to foster ROS accumulation in the water column. Because reduced P loading rates can contribute to excess nitrate accumulating in the water column of some lakes (Finlay et al. 2013) and would further encourage strict P-deficient growth conditions in lakes, current P-only management strategies may also exacerbate N stress occurrence in the future. Because stress regions were located within low mean annual precipitation regions, counter to expectations, we hypothesized that the temporal dynamics of nutrient delivery may influence N stress effects. Increased storm intensity is anticipated to create "flashier" systems, especially for those with existing subsurface tile drainage networks in the Corn Belt (Jaynes et al. 2001; David et al. 2010). Although N stress effects may be diminished during extended drought periods, buildup of inorganic and organic N in soils could result in large nitrate pulses to receiving waters during the next storm event (Gentry et al. 1998). For regions sharing landscape characteristics with the stress regions identified in this study, management agencies might want to consider strategies to reduce N and P export from watersheds and hydrologic modifications in watersheds to slow the delivery of large nutrient pulses to receiving waters. Additionally, our findings indicate that monitoring programs relying largely on Chl *a* or water transparency (i.e., Secchi depth) to characterize water quality in these regions may give a false sense of improved water quality. Instead, management agencies might want to consider additionally monitoring N, P, and nitrate concentrations frequently throughout the growing season and incorporating these results into water quality assessments.

References

Arbuckle, K. E., and J. A. Downing. 2001. The influence of watershed land use on lake N:P in a predominantly agricultural landscape. Limnol. Oceanogr. **46**: 970–975. doi: 10.4319/lo.2001.46.4.0970

Becher, K. D., S. J. Kalkhoff, D. J. Schnoebelen, K. K. Barnes, and V. E. Miller. 2001. Water-quality assessment of the eastern iowa basins-nitrogen, phosphorus, suspended sediment, and organic carbon in surface water, 1996-98. U.S. Geological Survey.

Bergström, A. K., and M. Jansson. 2006. Atmospheric nitrogen deposition has caused nitrogen enrichment and eutrophication of lakes in the northern hemisphere. Glob. Chang. Biol. **12**: 635–643. doi:10.1111/j.1365-2486.2006.01129.x

Bester, K., H. Huhnerfuss, U. Brockmann, and H. J. Rick. 1995. Biological effects of triazine herbicide contamination on marine phytoplankton. Arch. Environ. Contam. Toxicol. **29**: 277–283. doi:10.1007/BF00212490

Bracken, M. E. S., and others. 2015. Signatures of nutrient limitation and co-limitation: Responses of autotroph internal nutrient concentrations to nitrogen and phosphorus additions. Oikos **124**: 113–121. doi:10.1111/oik.01215

Bremigan, M. T., P. A. Soranno, M. J. Gonzalez, D. B. Bunnell, K. K. Arend, W. H. Renwick, R. A. Stein, and M. J. Vanni. 2008. Hydrogeomorphic features mediate the effects of land use/cover on reservoir productivity and food webs. Limnol. Oceanogr. **53**: 1420–1433. doi: 10.4319/lo.2008.53.4.1420

Brezonik, P. L., and J. Fulkerson-Brekken. 1998. Nitrate-induced photolysis in natural waters: Controls on

concentrations of hydroxyl radical photo-intermediates by natural scavenging agents. Environ. Sci. Technol. **32**: 3004–3010. doi:10.1021/es9802908

Canfield, Jr., D. E. 1983. Prediction of chlorophyll a concentrations in Florida lakes: The importance of phosphorus and nitrogen. J. Am. Water Resour. Assoc. **19**: 255–262. doi:10.1111/j.1752-1688.1983.tb05323.x

Cheruvelil, K. S., and others. 2017. Creating multithemed ecological regions for macroscale ecology: Testing a flexible, repeatable, and accessible clustering method. Ecol. Evol. **7**: 3046–3058. doi:10.1002/ece3.2884

Cooke, S. E., and E. E. Prepas. 1998. Stream phosphorus and nitrogen export from agricultural and forested watersheds on the Boreal Plain. Can. J. Fish. Aquat. Sci. **55**: 2292–2299. doi:10.1139/f98-118

Dai, G. Z., J. L. Shang, and B. S. Qiu. 2012. Ammonia may play an important role in the succession of cyanobacterial blooms and the distribution of common algal species in shallow freshwater lakes. Glob. Chang. Biol. **18**: 1571–1581. doi:10.1111/j.1365-2486.2012.02638.x

David, M. B., L. E. Drinkwater, and G. F. McIsaac. 2010. Sources of nitrate yields in the Mississippi River Basin. J. Environ. Qual. **39**: 1657–1667. doi:10.2134/jeq2010.0115

de Baar, H. J. W. 1994. von Liebig's law of the minimum and plankton ecology (1899–1991). Prog. Oceanogr. **33**: 347–386. doi:10.1016/0079-6611(94)90022-1

DeNoyelles, F., W. D. Kettle, and D. E. Sinn. 1982. The responses of plankton communities in experimental ponds to atrazine, the most heavily used pesticide in the United States. Ecology **63**: 1285–1293. doi:10.2307/1938856

Dillon, P. J., and F. H. Rigler. 1974. The phosphorus-chlorophyll relationship in lakes. Limnol. Oceanogr. **19**: 767–773. doi:10.4319/lo.1974.19.5.0767

Dinnes, D. L., D. L. Karlen, D. B. Jaynes, T. C. Kaspar, J. L. Hatfield, T. S. Colvin, and C. A. Cambardella. 2002. Review and interpretation: Nitrogen management strategies to reduce nitrate leaching in tile-drained midwestern soils. Agron. J. **94**: 153–171. doi:10.2134/agronj2002.0153

Donald, D. B., M. J. Bogard, K. Finlay, L. Bunting, and P. R. Leavitt. 2013. Phytoplankton-specific response to enrichment of phosphorus-rich surface waters with ammonium, nitrate, and urea. PLoS One **8**: e53277. doi:10.1371/journal.pone.0053277

Downing, J. A., and E. McCauley. 1992. The nitrogen:phosphorus relationship in lakes. Limnol. Oceanogr. **37**: 936–945. doi:10.4319/lo.1992.37.5.0936

Elser, J. J., E. R. Marzolf, and C. R. Goldman. 1990. Phosphorus and nitrogen limitation of phytoplankton growth in the freshwaters of North America: A review and critique of experimental enrichments. Can. J. Fish. Aquat. Sci. **47**: 1468–1477. doi:10.1139/f90-165

Elser, J. J., and others. 2009. Shifts in lake N:P stoichiometry and nutrient limitation driven by atmospheric nitrogen deposition. Science **326**: 835–837. doi:10.1126/science.1176199

Filstrup, C. T., T. Wagner, P. A. Soranno, E. H. Stanley, C. A. Stow, K. E. Webster, and J. A. Downing. 2014. Regional variability among nonlinear chlorophyll–phosphorus relationships in lakes. Limnol. Oceanogr. **59**: 1691–1703. doi:10.4319/lo.2014.59.5.1691

Filstrup, C. T., and J. A. Downing. 2017. Relationship of chlorophyll to phosphorus and nitrogen in nutrient-rich lakes. Inland Waters. doi:10.1080/20442041.2017.1375176

Finlay, J. C., G. E. Small, and R. W. Sterner. 2013. Human influences on nitrogen removal in lakes. Science **342**: 247–250. doi:10.1126/science.1242575

Fraterrigo, J. M., and J. A. Downing. 2008. The influence of land use on lake nutrients varies with watershed transport capacity. Ecosystems **11**: 1021–1034. doi:10.1007/s10021-008-9176-6

Gaynor, J. D., D. C. MacTavish, and W. I. Findlay. 1992. Surface and subsurface transport of atrazine and alachlor from a Brookston clay loam under continuous corn production. Arch. Environ. Contam. Toxicol. **23**: 240–245. doi:10.1007/BF00212282

Gelman, A., and J. Hill. 2007. Data analysis using regression and multilevel/hierarchical models. Cambridge Univ. Press.

Gentry, L. E., M. B. David, K. M. Smith, and D. A. Kovacic. 1998. Nitrogen cycling and tile drainage nitrate loss in a corn/soybean watershed. Agric. Ecosyst. Environ. **68**: 85–97. doi:10.1016/S0167-8809(97)00139-4

Glibert, P. M., J. Harrison, C. Heil, and S. Seitzinger. 2006. Escalating worldwide use of urea - a global change contributing to coastal eutrophication. Biogeochemistry **77**: 441–463. doi:10.1007/s10533-005-3070-5

Glibert, P. M., and others. 2016. Pluses and minuses of ammonium and nitrate uptake and assimilation by phytoplankton and implications for productivity and community composition, with emphasis on nitrogen-enriched conditions. Limnol. Oceanogr. **61**: 165–197. doi:10.1002/lno.10203

Guildford, S. J., and R. E. Hecky. 2000. Total nitrogen, total phosphorus, and nutrient limitation in lakes and oceans: Is there a common relationship? Limnol. Oceanogr. **45**: 1213–1223. doi:10.4319/lo.2000.45.6.1213

Hayes, N. M., M. J. Vanni, M. J. Horgan, and W. H. Renwick. 2015. Climate and land use interactively affect lake phytoplankton nutrient limitation status. Ecology **96**: 392–402. doi:10.1890/13-1840.1

Homer, C., and others. 2007. Completion of the 2001 National Land Cover Dataset for the conterminous United States. Photogramm. Eng. Remote Sensing **73**: 337–341.

Howarth, R. W., and others. 1996. Regional nitrogen budgets and riverine N & P fluxes for the drainages to the North Atlantic Ocean: Natural and human influences. Biogeochemistry **35**: 75–139. doi:10.1007/BF02179825

Jaynes, D. B., T. S. Colvin, D. L. Karlen, C. A. Cambardella, and D. W. Meek. 2001. Nitrate loss in subsurface drainage

as affected by nitrogen fertilizer rate. J. Environ. Qual. **30**: 1305–1314. doi:10.2134/jeq2001.3041305x

Jones, J. R., B. P. Borofka, and R. W. Bachmann. 1976. Factors affecting nutrient loads in some Iowa streams. Water Res. **10**: 117–122. doi:10.1016/0043-1354(76)90109-3

King, K. W., N. R. Fausey, and M. R. Williams. 2014. Effect of subsurface drainage on streamflow in an agricultural headwater watershed. J. Hydrol. **519**: 438–445. doi:10.1016/j.jhydrol.2014.07.035

Lapierre, J.-F., D. A. Seekell, C. T. Filstrup, S. M. Collins, C. E. Fergus, P. A. Soranno, and K. S. Cheruvelil. 2017. Continental-scale variation in controls of summer CO_2 in United States lakes. J. Geophys. Res. Biogeosci. **122**: 1–11. doi:10.1002/2016JG003525

Macrae, M. L., M. C. English, S. L. Schiff, and M. Stone. 2007. Intra-annual variability in the contribution of tile drains to basin discharge and phosphorus export in a first-order agricultural catchment. Agric. Water Manag. **92**: 171–182. doi:10.1016/j.agwat.2007.05.015

Martin, J. H., and S. E. Fitzwater. 1988. Iron deficiency limits phytoplankton growth in the north-east Pacific subarctic. Nature **331**: 341–343. doi:10.1038/331341a0

Martin, S. L., and P. A. Soranno. 2006. Lake landscape position: Relationships to hydrologic connectivity and landscape features. Limnol. Oceanogr. **51**: 801–814. doi:10.4319/lo.2006.51.2.0801

Marwood, C. A., R. E. H. Smith, J. A. Furgal, M. N. Charlton, K. R. Solomon, and B. M. Greenberg. 2000. Photoinhibition of natural phytoplankton assemblages in Lake Erie exposed to solar ultraviolet radiation. Can. J. Fish. Aquat. Sci. **57**: 371–379. doi:10.1139/f99-258

McCauley, E., J. A. Downing, and S. Watson. 1989. Sigmoid relationships between nutrients and chlorophyll among lakes. Can. J. Fish. Aquat. Sci. **46**: 1171–1175. doi:10.1139/f89-152

North, R. L., J. G. Winter, and P. J. Dillon. 2013. Nutrient indicators of agricultural impacts in the tributaries of a large lake. Inland Waters **3**: 221–234. doi:10.5268/IW-3.2.565

Odum, E. P., J. T. Finn, and E. H. Franz. 1979. Perturbation theory and the subsidy-stress gradient. Bioscience **29**: 349–352. doi:10.2307/1307690

Parker, A. E., R. C. Dugdale, and F. P. Wilkerson. 2012. Elevated ammonium concentrations from wastewater discharge depress primary productivity in the Sacramento River and the Northern San Francisco Estuary. Mar. Pollut. Bull. **64**: 574–586. doi:10.1016/j.marpolbul.2011.12.016

Peng, G., Z. Fan, X. Wang, and C. Chen. 2016. Photosynthetic response to nitrogen source and different ratios of nitrogen and phosphorus in toxic cyanobacteria, *Microcystis aeruginosa* FACHB-905. J. Limnol. **75**: 560–570. doi:10.4081/jlimnol.2016.1458

Plummer, M. 2012. JAGS Version 3.3.0 user manual. http://iweb.dl.sourceforge.net/project/mcmc-jags/Manuals/3.x/jags_user_manual.pdf

Prairie, Y. T., C. M. Duarte, and J. Kalff. 1989. Unifying nutrient–chlorophyll relationships in lakes. Can. J. Fish. Aquat. Sci. **46**: 1176–1182. doi:10.1139/f89-153

Sakamoto, M. 1966. Primary production by phytoplankton community in some Japanese lakes and its dependence on lake depth. Arch. Hydrobiol. **62**: 1–28.

Salin, M. L. 1988. Toxic oxygen species and protective systems of the chloroplast. Physiol. Plant. **72**: 681–689. doi:10.1111/j.1399-3054.1988.tb09182.x

Schilling, K. E., and M. J. Helmers. 2008. Effects of subsurface drainage tiles on streamflow in Iowa agricultural watersheds: Exploratory hydrograph analysis. Hydrol. Process. **22**: 4497–4506. doi:10.1002/hyp.7052

Schindler, D. W. 1977. Evolution of phosphorus limitation in lakes. Science **195**: 260–262. doi:10.1126/science.195.4275.260

Scott, J. T., and M. J. McCarthy. 2010. Nitrogen fixation may not balance the nitrogen pool in lakes over timescales relevant to eutrophication management. Limnol. Oceanogr. **55**: 1265–1270. doi:10.4319/lo.2010.55.3.1265

Smith, V. H. 1982. The nitrogen and phosphorus dependence of algal biomass in lakes: An empirical and theoretical analysis. Limnol. Oceanogr. **27**: 1101–1112. doi:10.4319/lo.1982.27.6.1101

Sommer, U. 1985. Comparison between steady state and non-steady state competition: Experiments with natural phytoplankton. Limnol. Oceanogr. **30**: 335–346. doi:10.4319/lo.1985.30.2.0335

Soranno, P. A., and others. 2015*a*. Building a multi-scaled geospatial temporal ecology database from disparate data sources: Fostering open science and data reuse. GigaScience **4**: 28. doi:10.1186/s13742-015-0067-4

Soranno, P. A., K. S. Cheruvelil, T. Wagner, K. E. Webster, and M. T. Bremigan. 2015*b*. Effects of land use on lake nutrients: The importance of scale, hydrologic connectivity, and region. PLoS One **10**: e0135454. doi:10.1371/journal.pone.0135454

Soranno, P. A., and others. 2017. LAGOS-NE: A multi-scaled geospatial and temporal database of lake ecological context and water quality for thousands of U.S. lakes. GigaScience, gix101. doi:10.1093/gigascience/gix101

Spiegelhalter, D., A. Thomas, N. Best, and D. Lunn. 2003. WinBUGS user manual, Version 1.4. MRC Biostatistics Unit.

Staehr, P. A., L. S. Brighenti, M. Honti, J. Christensen, and K. C. Rose. 2016. Global patterns of light saturation and photoinhibition of lake primary production. Inland Waters **6**: 593–607. doi:10.5268/IW-6.4.888

Stanley, E. H., and J. T. Maxted. 2008. Changes in the dissolved nitrogen pool across land cover gradients in Wisconsin streams. Ecol. Appl. **18**: 1579–1590. doi:10.1890/07-1379.1

Suttle, C. A., J. G. Stockner, and P. J. Harrison. 1987. Effects of nutrient pulses on community structure and cell size of a freshwater phytoplankton assemblage in culture. Can. J. Fish. Aquat. Sci. **44**: 1768–1774. doi:10.1139/f87-217

Takeda, K., H. Takedoi, S. Yamaji, K. Ohta, and H. Sakugawa. 2004. Determination of hydroxyl radical photoproduction rates in natural waters. Anal. Sci. **20**: 153–158. doi:10.2116/analsci.20.153

van der Ploeg, R. R., W. Böhm, and M. B. Kirkham. 1999. On the origin of the theory of mineral nutrition of plants and the Law of the Minimum. Soil Sci. Soc. Am. J. **63**: 1055–1062. doi:10.2136/sssaj1999.6351055x

Vidon, P., and P. E. Cuadra. 2010. Impact of precipitation characteristics on soil hydrology in tile-drained landscapes. Hydrol. Process. **24**: 1821–1833. doi:10.1002/hyp.7627

Vione, D., and others. 2006. Sources and sinks of hydroxyl radicals upon irradiation of natural water samples. Environ. Sci. Technol. **40**: 3775–3781. doi:10.1021/es052206b

Vitousek, P. M., and R. W. Howarth. 1991. Nitrogen limitation on land and in the sea: How can it occur? Biogeochemistry **13**: 87–115. doi:10.1007/BF00002772

Wagner, T., P. A. Soranno, K. E. Webster, and K. S. Cheruvelil. 2011. Landscape drivers of regional variation in the relationship between total phosphorus and chlorophyll in lakes. Freshw. Biol. **56**: 1811–1824. doi:10.1111/j.1365-2427.2011.02621.x

Yang, J., H. Lv, J. Yang, L. Liu, X. Yu, and H. Chen. 2016. Decline in water level boosts cyanobacteria dominance in subtropical reservoirs. Sci. Total Environ. **557–558**: 445–452. doi:10.1016/j.scitotenv.2016.03.094

Yang, J. R., H. Lv, A. Isabwe, L. Liu, X. Yu, H. Chen, and J. Yang. 2017. Disturbance-induced phytoplankton regime shifts and recovery of cyanobacteria dominance in two subtropical reservoirs. Water Res. **120**: 52–63. doi:10.1016/j.watres.2017.04.062

Yoshiyama, K., and J. H. Sharp. 2006. Phytoplankton response to nutrient enrichment in an urbanized estuary: Apparent inhibition of primary production by overeutrophication. Limnol. Oceanogr. **51**: 424–434. doi:10.4319/lo.2006.51.1_part_2.0424

Zafiriou, O. C. 1974. Sources and reactions of OH and daughter radicals in seawater. J. Geophys. Res. **79**: 4491–4497. doi:10.1029/JC079i030p04491

Acknowledgments

We thank members of the CSI Limnology Collaboration (www.csilimnology.org) for helpful comments during the framing, analysis, and drafting of this manuscript. Funding was provided by the National Science Foundation Macrosystems Biology Program through a collaborative grant to JAD (EF-1065649), EHS (EF-1065818), and Patricia A. Soranno (EF-1065786). SKO was funded by the University of Wisconsin Graduate School. Any use of trade, firm, or product names is for descriptive purposes only and does not imply endorsement by the U.S. Government. GLERL contribution number 1864.

Conflict of Interest

None declared.

Submitted 30 May 2017
Revised 29 September 2017
Accepted 04 October 2017

Associate editor: Yong Liu